第 36 卷第 1 期 无 机 化 学 学 报 Vol.36 No.1
2020 年 1 月 CHINESE JOURNAL OF INORGANIC CHEMISTRY 53-61

介孔 SBA-15 棒负载的 Pd_3Cl 催化剂催化 Sonogashira 偶联反应

何 蓉[1,2] 贠亚培[1,2] 孙莉莉[1,2] 盛鸿婷[1,2] 杜袁鑫[1,2] 项 东[1]
李 鹏*[,1,2] 袁孝友[1] 朱满洲*[,1,2] 洪 勋[3] 吴宇恩[3]
([1]安徽大学化学系,先进材料原子工程中心,
无机/有机杂化功能材料化学安徽省重点实验室,合肥 230601)
([2]安徽大学,杂化材料结构与功能调控教育部重点实验室,合肥 230601)
([3]中国科学技术大学化学系,先进纳米催化中心,合肥 230026)

摘要:通过静电吸引策略将具有高度分散性的原子精确纳米团簇$[Pd_3Cl(PPh_2)_2(PPh_3)_3]^+$($Pd_3Cl$)负载在介孔 SBA-15 棒上。结构明确的 Pd_3Cl/SBA-15 催化剂在以水作为溶剂以及温和的反应条件下对催化 Sonogashira 碳–碳偶联反应展现了较好的催化性能以及循环性。在此基础上,我们研究了 Pd_3Cl 团簇结构与性能之间的关系,并证实内核的 $Pd^{\delta+}$($0<\delta<2$)与配体之间的协同效应是催化反应的关键。

关键词:原子精确纳米团簇;SBA-15;静电吸引;Sonogashira 碳–碳偶联
中图分类号:TQ426.6;TQ426.65 **文献标识码**:A **文章编号**:1001-4861(2020)01-0053-09
DOI:10.11862/CJIC.2020.022

Mesoporous SBA-15 Rods Supported Pd_3Cl Catalysts for Sonogashira C-C Coupling

HE Rong[1,2] YUN Ya-Pei[1,2] SUN Li-Li[1,2] SHENG Hong-Ting[1,2] DU Yuan-Xin[1,2] XIANG Dong[1]
LI Peng*[,1,2] YUAN Xiao-You[1] ZHU Man-Zhou*[,1,2] HONG Xun[3] WU Yu-En[3]
([1]*Department of Chemistry and Centre for Atomic Engineering of Advanced Materials, Anhui Province Key Laboratory of Chemistry for Inorganic/Organic Hybrid Functionalized Materials, Anhui University, Hefei, Anhui* 230601, *China*)
([2]*Key Laboratory of Structure and Functional Regulation of Hybrid Materials* (*Anhui University*), *Ministry of Education, Hefei* 230601, *China*)
([3]*Center of Advanced Nanocatalysis* (*CAN*) *and Department of Chemistry, University of Science and Technology of China, Hefei* 230026, *China*)

Abstract: In this work, atomically precise $[Pd_3Cl(PPh_2)_2(PPh_3)_3]^+$ (denoted as Pd_3Cl) nanoclusters with high monodispersity were supported on the rod-like mesoporous SBA-15 by electrostatic attraction strategy. The well-defined Pd_3Cl/SBA-15 catalysts exhibited good catalytic performance and recyclability for Sonogashira C-C coupling reaction under mild condition with environment-friendly water as solvent. Importantly, we investigated the relationship between structures and properties of Pd_3Cl, which demonstrated that the synergistic effect between $Pd^{\delta+}$ ($0<\delta<2$) and the ligand was the key to the catalytic reaction.

Keywords: atomically precise nanoclusters; SBA-15; electrostatic attraction; Sonogashira C-C coupling

收稿日期:2019-09-22。收修改稿日期:2019-11-07。
国家自然科学基金(No.21571001,21372006,21631001,U1532141)基金资助项目。
*通信联系人。E-mail:peng-li@ahu.edu.cn,zmz@ahu.edu.cn

0 Introduction

C-C couplings of aryl halides containing Sonogashira, Suzuki and Heck coupling reactions have great significance for the development of organic chemistry[1-5]. To our knowledge, C(sp^2)-C(sp) bonds are usually intermediates or precursors for synthesizing natural products, bioactive drugs, and other materials[6-8]. Remarkably, one of the most common methods to form C(sp^2)-C(sp) bonds is Sonogashira coupling reaction[9-10]. The classic Pd(Ⅱ) complexes with Cu(Ⅰ) salt as co-catalysts have been employed to catalyze the Sonogashira reaction through homogeneous process such as $Pd(PPh_3)_2Cl_2$/CuI/Et_3N (Et_3N =triethylamine) combination[11]. Despite homogeneous catalysts exhibit superior catalytic activity, it remains challenging for the recovery and reuse of catalysts in which metal ions (*e.g.* Pd^{2+}, Cu^{+}) may contaminate the target products[9]. Subsequently, a series of palladium nanoparticles as heterogeneous catalysts have been designed and synthesized, which have potential to take the place of palladium complexes to solve these problems[12-14]. The use of supported catalysts shows growing importance for product purification and catalyst reuse. However, preparation of some supported catalysts is inefficient and the unclearly active sites of metal nanoparticles can complicate their catalytic mechanisms[15]. Therefore, simple and efficient methods are promising for preparing heterogeneous catalysts with definite structures. Fortunately, the atomically precise metal nanoclusters with well-defined structures can be chosen as model catalysts to provide a new perspective, which is helpful to understand the relationship between structures and properties at atomic level[16-18]. For example, Jin et al. reported that the Au_3 facet on spherical $Au_{25}(SR)_{18}$ and the waist sites of rod-shaped $Au_{25}(PPh_3)_{10}(C{\equiv}CPh)_5X_2$ were the active sites in catalytic the semihydrogenation of terminal alkynes[19]. Zhu′s group confirmed one-core-atom loss could boost hydroamination reaction of alkynes by comparing catalytic performance between Au_{25} and Au_{24} nanoclusters[20].

In addition, the harsher conditions are sometimes required in order to efficiently conduct Sonogashira cross-coupling reactions, such as high temperature[21-22], harmful solvents[23-25] and larger amount of catalysts[26]. Hence, the development of eco-friendly and moderate systems is also highly desirable.

In this work, atomically precise Pd_3Cl nanoclusters with positive charges and rod-shaped SBA-15 with negative charges are selected to fabricate well-defined Pd_3Cl/SBA-15 catalysts by electrostatic attraction strategy. The Pd_3Cl nanoclusters are successfully and readily supported on SBA-15 rods with high dispersity. The as-obtained Pd_3Cl/SBA-15 catalysts showed good catalytic activity by using water as green solvent at 55 ℃. The structure of Pd_3Cl nanoclusters consist of Pd_3 kernel protected by phosphine ligands and one chlorine atom. We demonstrated that the internal Pd atoms with positive charge due to bridging ligands can synergistically promote catalytic performance.

1 Experimental

1.1 Synthesis

1.1.1 Preparation of Pd_3Cl nanocluster

The Pd_3Cl clusters were achieved by modifying our previous strategy[27]. $PdCl_2$ (0.710 g, 4 mmol) was dissolved with hydrochloric acid (665 μL, 12 mol·L^{-1}), and the above solution was diluted to 5 mL with deionized water. 0.6 mL of as-prepared solution (0.6 mL, 0.48 mmol) was added into 10 mL of tetrahydrofuran (THF) containing triphenylphosphine (0.310 g, 1.2 mmol). After 10 minutes for vigorous stirring, $NaBH_4$ (80 mg, 2.1 mmol) dissolved in ethanol (5 mL) was added to the above solution. The reaction was maintained for 2 hours under vigorous stirring. The reaction solution was then centrifuged to remove the precipitate and evaporated the THF solvent with rotary evaporator. After that, the product was washed with ethanol for several times.

1.1.2 Preparation of SBA-15

4.0 g of copolymer P123 ($EO_{20}PO_{70}EO_{20}$, M_a=5 800) was dissolved with 30 mL water and HCl (120 mL, 2.0 mol·L^{-1}). After that, the above solution was stirred for 4 h. Subsequently, 8.5 g of TEOS (tetra ethyl oxysilane) was added and the solution was stirred at 1 100 r·

min^{-1} for 5 min. Then, the reaction system was kept for 24 h at 313 K. After that, the above solution was transferred to the Teflon-lined autoclave, and further treated at 403 K for 24 h. The final product was washed with water for several times, and calcined at 773 K for 6 h.

1.1.3　Preparation of the Pd_3Cl/SBA-15 catalysts

100 mg of SAB-15 was dispersed in CH_2Cl_2 (10 mL) under ultrasonication for a few minutes. 5 mg of Pd_3Cl nanoclusters in CH_2Cl_2 was added into to the above solution under magnetic stirring for 45 minutes. Pd_3Cl/SBA-15 catalysts were then obtained by centrifugation at 10 000 $r \cdot min^{-1}$.

1.2　Characterization methods

Silica gel 60 F254 and Merck Kieselgel 200-300 were chosen for analytical thin-layer chromatography (TLC) and prepared column chromatography. The yield was determined on Shimadzu GC 2010 plus by using flame ionization detector. UV-Vis spectra were measured on Techcomp UV1000 spectrophotometer from 300 to 700 nm. ^1H NMR and ^{13}C NMR spectra were recorded on a Bruker AM 400 spectrometer which were operated at 400 and 100 MHz respectively ($CDCl_3$ as solvent). The Fourier transform infrared (FT-IR) spectra were conducted on Bruker Tensor 27 instrument in the range of 4 000 ~200 cm^{-1}. Mass spectrometric analysis was performed by matrix-assisted laser desorption ionization mass spectrometry (MALDI-MS). The X-ray diffraction (XRD) patterns were recorded on SmartLab 9 KW with Cu $K\alpha$ radiation (λ=0.154 nm), and the 2θ range (40 kV and 100 mA) was from 10° to 90° in the step of 10°·min^{-1}. Transmission electron microscopy (TEM) and EDS (energy dispersive X-ray spectroscopy) mapping were performed in a JEM-2010 microscope with an accelerating voltage of 200 kV. X-ray photoelectron spectroscopy (XPS) measurements were acquired on ESCALAB 250Xi with Al $K\alpha$ radiation. Pd_3Cl nanoclusters loaded on the SBA-15 catalysts were measured by Inductively Coupled Plasma Mass Spectrometry (ICP-MS). ζ-potential analysis was determined by Malvern analyzer under an aqueous solution. Electrospray ionization mass spectrometry (ESI-MS) was recorded on MicroTOF-QIII high-resolution mass spectrometer, and the samples were infused into the chamber at 5 μL·min^{-1} directly. The N_2 adsorption/desorption isotherms were performed at liquid nitrogen temperature (−196 ℃) on a Micromeritics ASAP 2020M+C instrument, and the surface area of samples were calculated by Brunauer-Emmett-Teller (BET) theory.

1.3　Typical procedure for Sonogashira reaction

0.5 mmol phenylacetylene (55 μL), 0.5 mmol iodobenzene (56 μL), Pd_3Cl/SBA-15 catalysts (30 mg), and water (1 mL) were added into 10 mL shrek tube at 55 ℃ for 12 h in Ar. The final reaction product was obtained by centrifugation, and the yield was tested by GC (gas chromatography) equipment. The recovered catalyst was washed with *n*-hexane for next run under the same reaction conditions.

2　Results and discussion

2.1　Design and characterization of Pd_3Cl/SBA-15 catalyst

The Pd_3Cl/SBA-15 catalysts can be fabricated through electrostatic attraction between positively charged Pd_3Cl clusters and negatively charged SBA-15 rods (Scheme 1).

To demonstrate the feasibility of the proposed strategy, atomically precise Pd_3Cl nanoclusters were initially synthesized. UV-Vis spectrum of as-prepared Pd_3Cl nanoclusters (Fig.1a, the red line) exhibited three distinctive absorption peaks at about 340, 418, and 485 nm. As depicted in the matrix-assisted laser desorption ionization mass spectrum (MALDI-MS), the as-obtained Pd_3Cl nanoclusters present a molecular ion peak at 1 511 (*m*/*z*) (theoretical M_w=1 511), and two fragments were captured for losing of the PPh_3 units (Fig.1b, the blue line). TEM shows that the average size of as-prepared Pd_3Cl clusters is around 1.4 nm (Fig.2a) and the size distribution pattern was shown in Fig.S1. In addition, Pd_3Cl were maintained at 150 ℃ in Ar to test the thermal stability. Notably, the UV-Vis spectrum of the Pd_3Cl nanocluster after thermal treatment is same to that of fresh Pd_3Cl nanocluster (Fig.1a, the blue line). The MALDI-MS

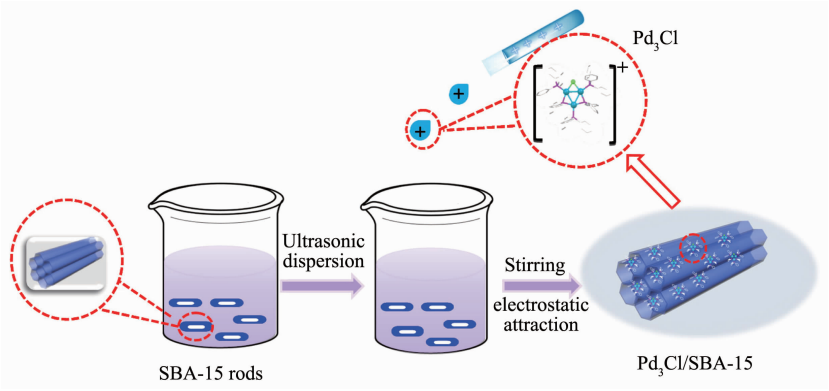

Scheme 1 Schematic illustration for the formation of Pd_3Cl/SBA-15 by electrostatic attraction strategy

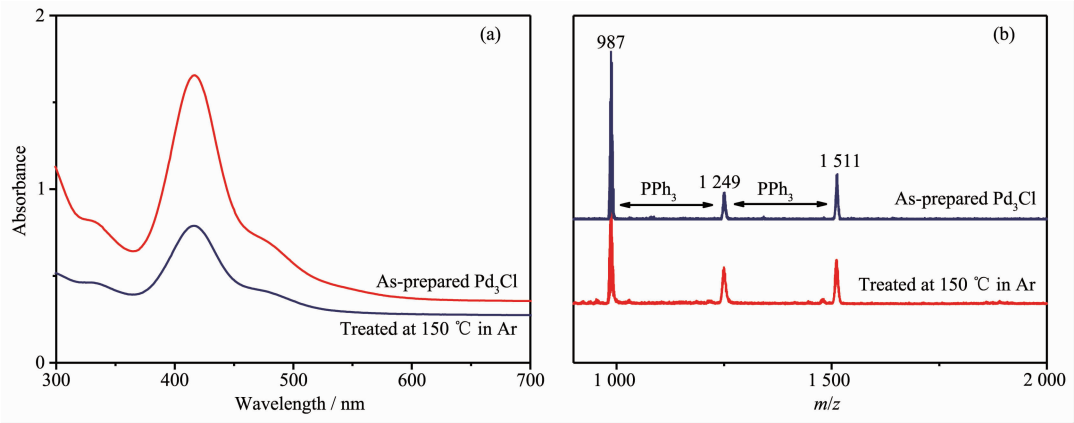

Fig.1 (a) UV-Vis absorption spectra of the as-prepared Pd_3Cl nanocluster (in dichloromethane, red line) and the redissolved nanoclusters after thermal treatment at 150 ℃ in Ar for 1 h (blue line); (b) Positive mode MALDI mass spectrum of as-prepared Pd_3Cl nanocluster and after thermal treatment, the peak except the position of 1511 is the fragment of Pd_3Cl

analysis also showed a sharp peak at 1 511 (*m*/*z*) after thermal treatment (Fig.1b, the red line). Therefore, Pd_3Cl possessed good thermal stability and the structure of Pd_3Cl remained intact in the process of anneal treatment.

Furthermore, the synthesis of SBA-15 materials followed the previously reported procedure[28]. The SEM (Fig.2b) and TEM (Fig.S2) images show that the as-prepared SBA-15 present rode-like morphologies with well-ordered mesoporous structures. As displayed in Fig.S3, the broad diffraction peak of SBA-15 was assigned to the characteristic peak of amorphous silica. The surface ζ potential of SBA-15 showed −20.1 mV that evidenced SBA-15 with negative charge surface (Fig.S4).

To obtain further insight into the catalysts, various characterization techniques were employed to determine the as-prepared Pd_3Cl/SBA-15 samples. The elemental maps of Si, O and Pd of Pd_3Cl/SBA-15 catalyst were shown in Fig.2c. From the elements mapping, Pd_3Cl nanoclusters were uniformly dispersed on a SBA-15 support by electrostatic attraction strategy. The loading of catalyst is 0.8% (*w*/*w*) palladium by Inductively Coupled Plasma Mass Spectrometry (ICP-MS). No obvious change was observed from the XRD pattern after Pd_3Cl loading, which suggests that the SBA-15 rods are chemically stable (Fig.S3). The XPS directly illustrates the inexistence of any interaction between Pd_3Cl nanoclusters and SBA-15 supports during loading, for the reason that the Pd3*d* bond energy (Pd_3Cl/SBA-15) agreed well with that of fresh Pd_3Cl (Fig.S5). The Fourier transform infrared spectroscopy (FT-IR) confirmed the successful fusion of Pd_3Cl and SBA-15 (Fig.S6). N_2 adsorption and

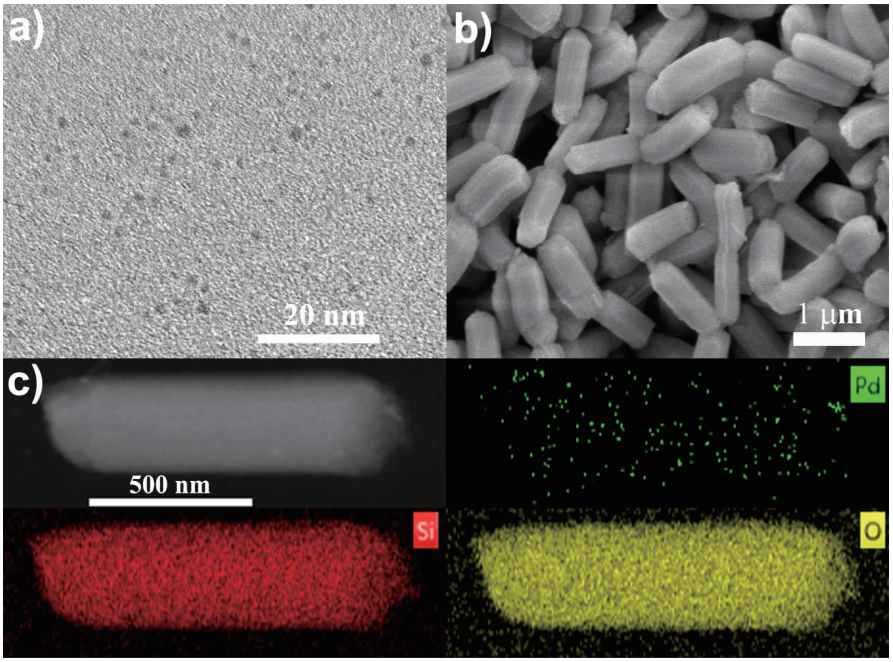

Fig.2　(a) TEM image of as-prepared Pd_3Cl nanoclusters; (b) SEM image of the as-obtained SBA-15 rods; (c) EDS elemental mapping images of the as-prepared Pd_3Cl/SBA-15 catalysts

desorption Isotherms of SBA-15 and Pd_3Cl/SBA-15 catalyst were shown in Fig.S7. The BET surface area of SBA-15 rod was determined to be 588 $m^2 \cdot g^{-1}$, which decreased to 468 $m^2 \cdot g^{-1}$ after the loading of Pd_3Cl nanoclusters. In general, the structural integrity of Pd_3Cl nanoclusters supported on SBA-15 was maintained.

2.2　Catalytic properties of Pd_3Cl/SBA-15 for sonogashira C-C coupling

We selected Sonogashira C-C coupling as a model reaction to explore the catalytic performance of the as-synthesized Pd_3Cl/SBA-15 catalysts. To increase sustainability of the reaction system, water was used as environment-friendly solvent. Next, the impact of diversified bases was initially evaluated. We found that the reaction activity reached only 20% / 25% using K_2CO_3 or Cs_2CO_3 as base at 65 ℃ (Table 1, entries 1 ~2), and without base, products were not detected (Table 1, entry 3). Interestingly, the yield was markedly improved to 90% in the presence of Et_3N as a base (Table 1, entry 4). The highest yield (92.8%) was achieved when the temperature decreased to 55 ℃ (Table 1, entry 5). However, with a further decrease in temperature, the activity was obviously decreased to 72% (Table 1, entry 7). Under optimal temperature (55 ℃), 82.4% of product was produced with pyrrolidine as base (Table 1, entry 6). Then, 10 or 20 mg of Pd_3Cl/SiO_2 were used, and the lower yield was produced (Table 1, entries 8~9). Eventually, entry 5 of Table 1 was chose as the optimum conditions for Pd_3Cl/SBA-15-catalyzed Sonogashira reaction. For comparison, we also investigated the catalytic activity of Pd_3Cl/CeO_2 catalyst, which have a lower yield (88%, Table 1, entry 10) than that of Pd_3Cl/SBA-15 catalyst (92.8%, Table 1, entry 5). We also directly grew ZIF-8 outside the heterogeneous Pd_3Cl/CeO_2 catalyst (denoted as Pd_3Cl/CeO_2@ZIF-8). The yield (77%, Table 1, entry 11) was lower than that of Pd_3Cl/CeO_2 catalysts. Because the small ZIF-8 cores (<2 nm) limited the access of reactants to Pd_3Cl nanoclusters and the diffusion of reactants inside the ZIF-8 pores[29]. The TEM image of Pd_3Cl/SBA-15@ZIF-8 was shown in Fig.S8. It was worth noting that no product was observed in blank experiments, in which Pd_3Cl nanoclusters were absent and SBA-15 or CeO_2 oxide were present (Table 1, entry 12~13). This demonstrated that catalytic activity arose out of the Pd_3Cl nanoclusters.

Table 1 Sonogashira cross-coupling reaction with Pd_3Cl/SAB-15 and related catalysts[a]

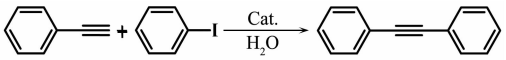

Entry	Catalyst	Temperature / ℃	Base	Yield / %[b]
1	Pd_3Cl/SBA-15	65	K_2CO_3	20
2	Pd_3Cl/SBA-15	65	Cs_2CO_3	25
3	Pd_3Cl/SBA-15	65	none	n.r.
4	Pd_3Cl/SBA-15	65	Et_3N	90
5	Pd_3Cl/SBA-15	55	Et_3N	92.8
6	Pd_3Cl/SBA-15	55	C_4H_9N	82.4
7	Pd_3Cl/SBA-15	40	Et_3N	72
8	Pd_3Cl/SBA-15	55	Et_3N	87[c]
9	Pd_3Cl/SBA-15	55	Et_3N	85[d]
10	Pd_3Cl/CeO_2	55	Et_3N	88
11	Pd_3Cl/CeO_2@ZIF-8	55	Et_3N	77
12	SBA-15	55	Et_3N	n.r.[e]
13	CeO_2	55	Et_3N	n.r.[f]
14	Pd_3Cl/SBA-15-400	55	Et_3N	67
15	Pd_3Cl/CeO_2-400	55	Et_3N	71

[a] Reaction conditions: iodobenzene (0.5 mmol), phenylacetylene (0.5 mmol), base (1 mmol), H_2O (1 mL), 12 h, 30 mg catalyst, 0.8%(*w*/*w*) of palladium, 0.753 μmol of Pd_3Cl, 1.4×10^{-5} (*n*/*n*) of substrate; [b] Yield was detected by GC; [c] 20 mg of Pd_3Cl/SiO_2; [d] 10 mg of Pd_3Cl/SiO_2; [e] 30 mg SBA-15 was used, n.r.=no reaction; [f] 30 mg CeO_2 was used

2.3 Scope of the catalytic reaction: derivatives of aryl iodide and phenylacetylene

In order to further evaluate Pd_3Cl/SBA-15 catalysts, we extended the study to different combinations of aryl iodides and alkynes under the optimized conditions. Whatever electron-rich or electron-poor phenylacetylene derivatives showed satisfactory yield (Table 2, entries 1~3). Both iodobenzene with electron-withdrawing and that with electron-donating groups were examined. Notice that, aryl iodide with withdrawing group showed excellent yields (93.4%, Table 2, entry 4). In contrast, when iodobenzene was attached with the electron-donating group, the yield varied from 93.4% to 81.3% (Table 2, entry 5). Lower activity

Table 2 Catalytic performance of difference substrates with Pd_3Cl/SBA-15[a]

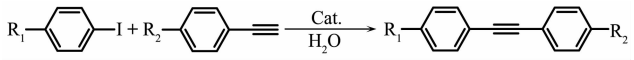

Entry	Aryl halide	Terminal alkyne	Product	Yield[b] / %
1	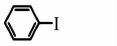	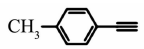	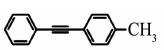	90.3
2	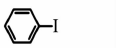	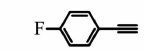	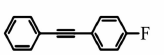	91.2
3	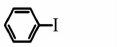	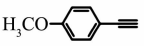	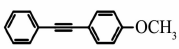	88.5
4	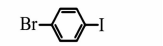		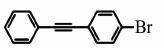	93.4
5	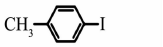		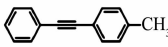	81.3
6	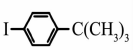	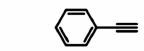	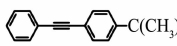	67.1

[a] Reaction conditions: 30 mg Pd_3Cl/SBA-15 catalyst, 0.5 mmol aryl halide, 0.5 mmol terminal alkyne, 1 mL H_2O, 55 ℃ reaction temperature, 12 h; [b] Yield was detected by GC

(67.1%, Table 2, entry 6) was observed when iodobenzene with stronger electron-donating group for Sonogashira coupling reaction.

The recyclability of the Pd_3Cl/SBA-15 catalyst was examined (Fig.3). In this test, the Pd_3Cl/SBA-15 catalyst was recovered by centrifugation after Sonogashira reaction for next run. We found that the activity of the catalyst decreased only 8% even after eight cycles, which suggested the high stability of the designed catalyst based on electrostatic attraction strategy.

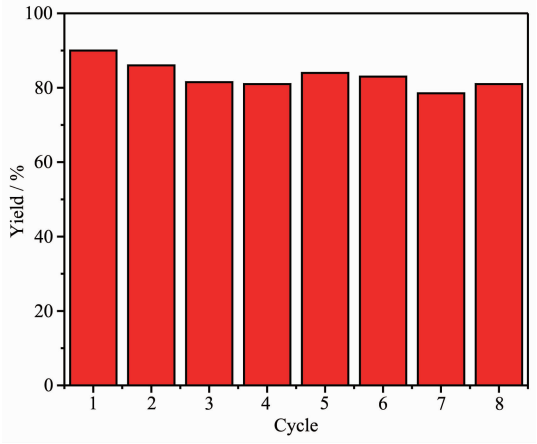

Fig.3　Recyclability of Pd_3Cl/SBA-15 catalyst in Sonogashira C-C coupling reaction

2.4　Evidence for the importance of structural integrity of Pd_3Cl nanocluster

To understand the nature of Pd_3Cl/SBA-15 catalysts after reaction, several experiments were performed. Any shift of Pd3*d* energy was not observed from XPS spectra (Fig.S5). The XRD patterns (Fig.S3) and FT-IR spectra (Fig.S6) also remained almost unchanged before and after reaction, indicating the integrity of Pd_3Cl nanocluster was preserved during reaction process.

To further reveal the relationship between catalytic property and structure of nanocluster, Pd_3Cl/SBA-15 catalysts were calcined at 400 ℃ in Ar atmosphere. It was worth mentioned that the activity decreased to 67% after calcination at 400 ℃ (Table 1, entry 14). Not surprisingly, similar results were observed when calcined Pd_3Cl/CeO_2 at 400 ℃ (71%, Table 1, entry 15).

Furthermore, the binding energy of Pd3$d_{5/2}$ (as-prepared Pd_3Cl/SBA-15) was 337.1 eV from XPS result and agree well with the fresh Pd_3Cl nanocluster, indicating that Pd was positively charged due to the interaction between Pd and the ligands (Fig.4(a, b)). The bond energy of Pd3$d_{5/2}$ decreased to 335.9 eV after calcination Pd_3Cl/SBA-15 at 400 ℃ from XPS spectrum (Fig.4c). According to previous report, we classified 335.9 eV as the binding energy of Pd(0), which indicated that the ligands on the surface of Pd_3Cl nanocluster were removed and $Pd^{\delta+}$ were reduced to a metallic state, while the Pd3$d_{5/2}$ peak at 337.5 eV was assigned to Pd^{2+}[30]. Meanwhile, we also found that Pd(0) was produced from the XRD pattern (Fig.5), in which the position of 40° was the (111) plane of Pd(0) (PDF No.88-2335)[31]. Both of these suggested the Pd(0) atoms were exposed on the cluster surface through

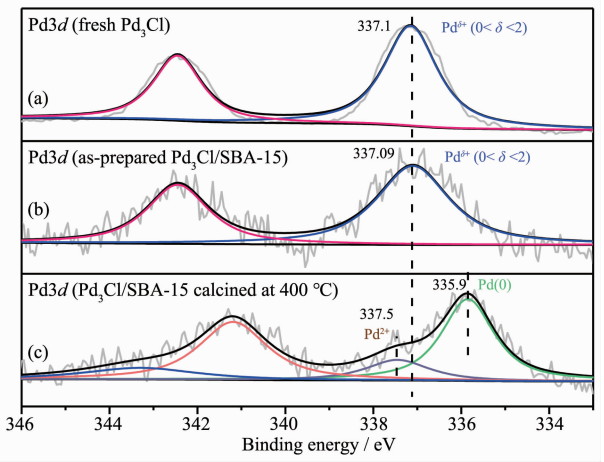

Fig.4　XPS spectra in Pd3*d*: (a) Fresh Pd_3Cl/SBA-15 catalyst; (b) As-prepared Pd_3Cl/SBA-15; (c) Pd_3Cl/SBA-15 calcined by 400 ℃

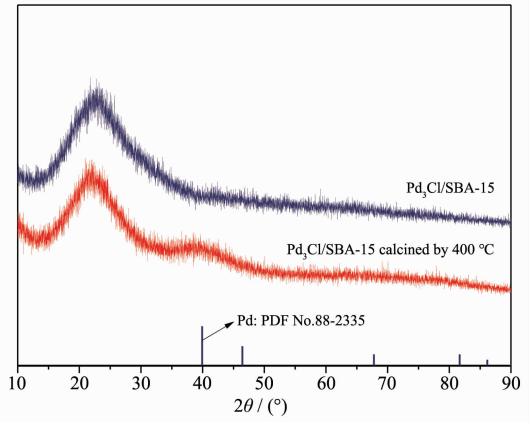

Fig.5　XRD patterns of Pd_3Cl/SBA-15 and Pd_3Cl/SBA-15 calcined by 400 ℃

heat treatment, which were responsible for the decrease in activity. However, this was contrary to the conventional opinion that the higher catalytic performance could be obtained when more surface atoms were bare[32]. The above results indicated the importance of intact structure of Pd_3Cl nanocluster for catalytic performance. The synergistic effect between $Pd^{\delta+}$ ($0<\delta<2$) and the ligand is the key to the catalytic reaction.

We tried to investigate the catalytic process of Sonogashira cross-coupling reaction through homogeneous Pd_3Cl nanocluster. The FT-IR spectra of phenylacetylene+Pd_3Cl+Et_3N were investigated (Fig. S9), the C≡C stretching increased from 2 111 to 2 118 cm^{-1} and the position of C≡C-H stretching disappeared. This suggests that the H atom from C≡C-H group is removed and then may interact with the nanocluster to form an intermediate[33]. Furthermore, the Electrospray mass spectrometry (ESI-MS) was adopted for insight into the intermediate. In the presence of Et_3N, Pd_3Cl can interact with phenylacetylene, and new peak appear at m/z=1 577.1 referred to $Pd_3\cdots C\equiv C-Ph$, and the simulation result agree well with experimental result (Fig.S10). Based on above experimental results and previous reports[27], the terminal alkyne may be activated with a base for forming $Pd_3\cdots C\equiv C-Ph$, which further interacted with iodobenzene to generate products.

3 Conclusions

Well-defined Pd_3Cl/SBA-15 catalysts have been designed and readily synthesized by electrostatic attraction between positively charged atomically precise Pd_3Cl clusters and negatively charged mesoporous SBA-15 rods. It was found that the recyclable heterogeneous Pd_3Cl/SBA-15 catalysts were robust, stable, and presented efficient catalytic activities for the water-mediated Sonogashira C-C coupling reaction. We demonstrated the structure integrity of Pd_3Cl and the synergistic effect between the ligand and $Pd^{\delta+}$ ($0<\delta<2$) are key for the excellent stability and high activity in Sonogashira reaction. This synthetic strategy may also be applicable to design other atomically precise metal cluster-based heterogeneous catalysts.

Conflict of interest: The authors declare that they have no conflict of interest.

Supporting information is available at http://www.wjhxxb.cn

References:

[1] Chinchilla R, Najera C. *Chem. Rev.*, **2007**,**107**(3):874-922

[2] Biffis A, Centomo P, Zotto A D, et al. *Chem. Rev.*, **2018**,**118**(4):2249-2295

[3] Chinchilla R, Najera C. *Chem. Rev.*, **2014**,**114**(3):1783-1826

[4] Yuan B Z, Pan Y Y, Li Y W, et al. *Angew. Chem. Int. Ed.*, **2010**,**49**(24):4054-4058

[5] Lin J Z, Abroshan H, Liu C, et al. *J. Catal.*, **2015**,**330**:354-361

[6] Paterson I, Davies R D M, Marquez R. *Angew. Chem. Int. Ed.*, **2001**,**40**(3):603-607

[7] Bagley M C, Dale J W, Merritt E A, et al. *Chem. Rev.*, **2005**,**105**(2):685-714

[8] Brunsveld L, Meijer E W, Prince R B, et al. *J. Am. Chem. Soc.*, **2001**,**123**(33):7978-7984

[9] Karak M, Barbosa L C A, Hargaden G C. *RSC Adv.*, **2014**,**4**(96):53442-53466

[10]Nicolaou K C, Bulger P G, Sarlah D. *Angew. Chem. Int. Ed.*, **2005**,**44**(29):4442-4489

[11]Dissanayake K C, Ebukuyo P O, Dhahir Y J, et al. *Chem. Commun.*, **2019**,**55**(34):4973-4976

[12]Kozell V, McLaughlin M, Strappaveccia G, et al. *ACS Sustainable Chem. Eng.*, **2016**,**4**(12):7209-7216

[13]Seth J, Kona C N, Das S, et al. *Nanoscale*, **2015**,**7**(3):872-876

[14]Elhage A, Lanterna A E, Scaiano J C. *ACS Sustainable Chem. Eng.*, **2018**,**6**(2):1717-1722

[15]Zhang X Y, Sun Z C, Wang B, et al. *J. Am. Chem. Soc.*, **2018**,**140**(3):954-962

[16]Zhou Y, Li G. *Acta Phys. Chim. Sin.*, **2017**,**33**(7):1297-1309

[17]Chakraborty I, Pradeep T. *Chem. Rev.*, **2017**,**117**(12):8208-8271

[18]Jin R C, Zeng C J, Zhou M, et al. *Chem. Rev.*, **2016**,**116**(18):10346-10413

[19]Li G, Jin R C. *J. Am. Chem. Soc.*, **2014**,**136**(32):11347-11354

[20]Wang L Q, Shen K Q, Chen M Y, et al. *Nanoscale*, **2019**,**11**(29):13767-13772

[21]Yin L X, Liebscher J. *Chem. Rev.*, **2007**,**107**(1):133-173

[22]Tukhani M, Panahi F, Khalafi-Nezhad A. *ACS Sustainable Chem. Eng.*, **2018**,**6**(1):1456-1467

[23]Li G, Jiang D E, Liu C, et al. *J. Catal.*, **2013**,**306**:177-183

[24]Gholinejad M, Bahrami M, Nájera C, et al. *J. Catal.*, **2018**, **363**:81-91

[25]Moon J, Jang M, Lee S. *J. Org. Chem.*, **2009**,**74**(3):1403-1406

[26]Li Z M, Yang X J, Liu C, et al. *Prog. Nat. Sci.*: *Mater. Int.*, **2016**,**26**(5):477-482

[27]Fu F Y, Xiang J, Cheng H, et al. *ACS Catal.*, **2017**,**7**(3):1860-1867

[28]Wang Q, Wang Z C, Zheng T H, et al. *Nano Res.*, **2016**,**9**(8):2294-2302

[29]Teng J, Chen M Q, Xie Y Y, et al. *Chem. Mater.*, **2018**,**30**(18):6458-6468

[30]Li Z P, Yang X C, Tsumori N, et al. *ACS Catal.*, **2017**,**7**(4):2720-2724

[31]Wang Z C, Chen W, Han Z L, et al. *Nano. Res.*, **2014**,**7**(9):1254-1262

[32]Li Q, Das A, Wang S X, et al. *Chem. Commun.*, **2016**,**52**(99):14298-14301

[33]Liu Y Y, Chai X Q, Cai X, et al. *Angew. Chem. Int. Ed.*, **2018**,**57**(31):9775-9779